Special Issue on "Innovative Technologies for Industrial Waste Management"
J. Indian Chem. Soc.,
Vol. 97, No. 9a, September 2020, pp. 1391-1398

A comparative study on Cr(VI) removal by graphene oxide (GO) and functionalized reduced graphene oxide (fRGO)

Spandan Ghosh*, Soumya Kanta Ray and Chanchal Majumder[c]

Department of Civil Engineering, Indian Institute of Engineering Science and Technology, Shibpur, Howrah-711 103, West Bengal, India

E-mail: sgcoolspandan@gmail.com

Manuscript received online 09 January 2020, accepted 26 June 2020

Effluent mainly from metal processing industry contains toxic hexavalent chromium is a major concern. In this study Cr^{6+} removal was done by graphene oxide (GO) and iron functionalized reduced graphene oxide (fRGO) and a comparative study was carried out. At equilibrium pH 2, fRGO gives more removal than GO. For both the materials, Langmuir adsorption isotherm fit better than Freundlich isotherm. The adsorption capacities of GO and fRGO are found to be (9.90 mg g^{-1}) and (17.54 mg g^{-1}) respectively. The Langmuir adsorption isotherm constants for GO and fRGO (K_L) are found to be (32.90) and (24.08) respectively. Both the materials follow pseudo-second order removal kinetics and fRGO (0.07 g mg^{-1} min^{-1}) shows faster removal rate than GO (0.03 g mg^{-1} min^{-1}). It was found that (fRGO) can remove 1.77 times more Cr^{6+} than graphene oxide (GO). The material can remove 97.22% Cr^{6+} at optimum pH of 2 and at fRGO dose of 100 mg/100 mL. The method can be used for treating acidic chrome bath effluent effectively.

Keywords: Chromium, comparative study, adsorption, GO, fRGO.

Introduction

Chromium occurs mostly in the form of trivalent chromium [Cr(III)] and hexavalent chromium [Cr^{6+}] in the aqueous medium. These two oxidation conditions of chromium have dissimilar biological, chemical and environmental properties[1]. Cr^{6+} is 500 times more noxious than Cr(III)[2]. Trivalent chromium [Cr^{3+}] is insoluble and this is also an essential micro nutrient[3], whereas hexavalent chromium is highly toxic and portable in the environment which act as mutagens, carcinogens, teratogens[4].

Chromium(III) is discharged mostly from industries such as leather tanning, lubricant, pesticides, textile dyeing, mining, and electroplating[5,6]. In third world countries the industrial discharges are directed towards different water bodies with different level of contamination. Mostly the discharge from tanning industries contained chromium enhanced tanning process for its processing speed, greater stability of resulting leather and low cost. In leather tanning process leather only takes up 60–80% of chromium and the rest is discharged into water which causes a serious environmental problem[7]. USEPA has recommended the value of chromium is 0.1 ppm in drinking water[8]. Permissible limit for Cr^{3+} and Cr^{6+} in wastewater are 5 mg L^{-1} and 0.5 mg L^{-1} respectively[6,9]. Several methods have been built up for the removal of Cr^{6+} such as electro-chemical precipitation[10], cyanide treatment[11], reverse osmosis[12], ion exchange[13,14], adsorption[15,16]. Among these methods, adsorption is mostly used because of its low cost due to regeneration of adsorbents which solves sludge disposal problems[17–20]. The lubricant manufacture industry produced highly hydrophobic solution of waste that reduced dissolve oxygen rapidly. Pesticide industry discharged recalcitrant outcome that is not biodegradable very easily. Textile and electroplating industry produced heavy metal contaminants those are mutate aqua life[6].

Since the innovation of buckyballs by curl korto and smalley, a rapidly increasing new field, nanotechnology, was developed[21]. Firstly, nanotechnology was used for medicine, electronics and biotechnology. But recently it is seen that it is also beneficial in the case of water treatment[22]. Nanoparticles can show an array of novel properties, because of its small size, which is responsible for development of new technology and improvement of existing one[23].

Graphene is a two-dimensional structure which consists of sp^2-hybrid carbons, containing only one atomic thickness and used for electronic, magnetic, power storage, water and wastewater treatment[24]. Synthesis of this graphene oxide reported elaborately elsewhere[25]. This study functionalized reduced graphene oxide (fRGO) was prepared by impregnation of iron into reduced graphene oxide (RGO)[26]. The aim of this research is to carry out a comparative study between GO and fRGO for Cr^{6+} removal from contaminated water.

Materials and methods

Reagents:

Different chemicals such as powdered graphite, sodium nitrate ($NaNO_3$), conc. sulphuric acid (H_2SO_4), hydrazine hydrate N_2H_4 (50–60%) and *N,N*-dimethylformamide (DMF) are procured from Merck, Dermasdat, Germany.

Synthesis of GO and fRGO:

Graphene oxide (GO) was synthesized via Hummer's method[25]. For his study, 5 g of graphite powder (Mesh size 60) and 2.5 g $NaNO_3$ was mixed. Within this mixture 120 mL concentrated H_2SO_4 was added dropwise and a magnetic stirrer (Tarson, India) at 500 rpm was used to mix the content in 1 L borosil glass beaker. To control the reaction temperature the glass beaker was kept into an ice bath. When vigorous stirring was continuing, 15 g $KMnO_4$ was added in very control manner so that the temperature of this solution is maintained below 20°C. After that the solution was removed from ice bath and stirred at 35°C for half an hour. At the time of reaction, the solution become pasty, the colour transformed to light brown. Temperature of this mixture was raised to 98°C and it was retained for 15 min by heating externally. After stopped the heating, the pasty compound was cooled in a water bath for 20 min. To stop the oxidation process 450 ml deionized (DI) water is used. 15 mL aliquot H_2O_2 was mixed to the mixture, and the colour changed to yellowish. The solution is then washed and centrifuged several times with 10% HCl and DI water at pH 7.

The powdered GO was dispersed in DI water. Hydrazine hydrate was mixed in the solution and heated for 2 h at 100°C with stirring. The mixture was then brought in a water-cooling condenser. After 24 h, black solid precipitation was formed as a reduced graphene oxide (RGO). *N,N*-Dimethylformamide (DMF) was mixed with the solution at DMF/H_2O ratio 9:1. From this a mixture of 3 mL was dispersed in DI water and 15 mg $FeSO_4.7H_2O$ was added in this dispersion. The solution was mixed for 24 h at 27°C. After 24 h, 5 mL of 0.1 *N* NH_4OH was mixed until the pH was achieved 8 and the colour changes to deep brownish red which signifies formation of ferric hydroxide. The precipitate was filtered and dried in oven at 85°C for 12 h to get fRGO[26] and characterization is done elsewhere. With the as-synthesized material the effect of different parameter such as pH, dose of adsorbent and kinetic study was done. The Cr^{6+} solution is prepared by dissolving potassium di-chromate ($K_2Cr_2O_7$) in DI water and was determined colorimetric method as per Standard Methods (1995).

Experimental

Effect of pH:

Batch studies were performed to calculate percentage removal of Cr^{6+} at varying pH values. For studying effect of adsorption on Cr^{6+} removal at different pH, six trial solutions are prepared by adjusting the pH 2, 4, 6, 8, 10, 12 respectively with the help of 0.25 *N* NaOH solution and 0.25 *N* HCl solution for each adsorbent. After that, 10 mg of adsorbents are mixed with 100 mL of 0.2 mg/L of prepared Cr^{6+} solution. The solutions were kept in the shaker and shaken at 150 rpm for 4 h at 27°C. The samples were filtered and resulting Cr^{6+} concentration of filtrate was computed. Final pH after the adsorption is measured to obtain the value close to equilibrium pH.

Effect of dose of adsorbent:

Batch adsorption experiment were performed with various doses of GO and fRGO. To analyse the effect of doses on Cr^{6+} removal, five different solution of adsorbents doses 10 mg, 20 mg, 40 mg, 60 mg, 80 mg, 100 mg respectively are added in 100 mL of 0.2 mg/L of Cr^{6+} synthetic solution for both the adsorbents. Adjust the pH to equilibrium pH which is approximately 2 of all the solutions. The samples were then shaken at 150 rpm for 4 h at 27°C. Then the solutions were passed through 0.45 μm filter paper.

Effect of time:

Batch kinetics were performed with equilibrium dose of about 100 mg of GO and fRGO in 100 mL of 0.2 mg/L of Cr^{6+} sample. Set the pH to the equilibrium pH of about 2 of all samples. The samples were then shaken at varying time

period from 10 min, 30 min, 60 min, 90 min, 120 min, 150 min, 180 min, 240 min respectively. Eight different trial solutions were analysed for each case at varying time interval at 27°C and filtered using 0.45 μm filter paper.

Results and discussion

Characterization of nano-material:

The reduced graphene oxide (RGO) and iron functionalized reduced graphene oxide (fRGO) are characterized by Fourier transform infrared spectroscopy (FTIR) to identify the functional groups associated with RGO and fRGO and presented in Fig. 1.

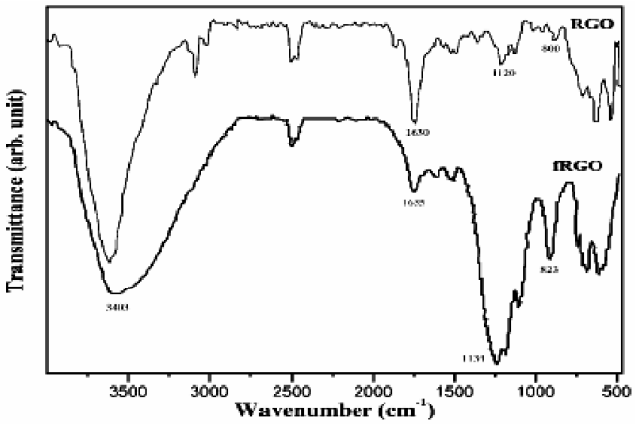

Fig. 1. Fourier transform infrared spectroscopy (FTIR) of RGO and fRGO (Aadopted from Ref. 26).

The main functional group are presents are carboxyl (-COOH), carbonyl (C=O) and hydroxyl (-OH). The functional groups and iron functionalization are enhanced the chemisorption of Cr^{6+} from contaminated water[26].

Effect of pH:

pH is an essential aspect that influences the amount and nature of surface charge of adsorbent. The effect of pH on adsorption of Cr^{6+} is shown in the Fig. 2 and Tables 1(a) and Table1(b).

Maximum adsorption took place at pH 2 for both the adsorbents (GO and fRGO). Results shows that at equilibrium pH (2±0.2), Cr^{6+} removal efficiency on GO and fRGO is 54% and 66% respectively. As the pH value increased, the % removal is decreased.

It is reported that there are several functional groups such as -COOH and -OH exist on the surface of graphene oxide

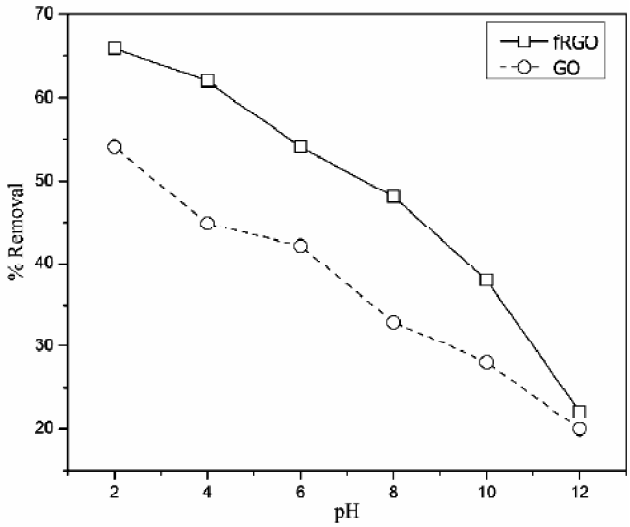

Fig. 2. Effect of pH on Cr^{6+} removal (%).

Table 1(a). Effect of pH on Cr^{6+} removal (%) by GO

Sl. no.	pH	Initial conc. of Cr^{6+} (mg/L)	Average effluent conc. of Cr^{6+} (mg/L)	Adsorbed conc. of Cr^{6+} (mg/L)	Cr^{6+} removal (%)
1.	2	0.2	0.092	0.108	54.10
2.	4	0.2	0.110	0.090	44.88
3.	6	0.2	0.116	0.084	42.12
4.	8	0.2	0.134	0.066	32.90
5.	10	0.2	0.144	0.056	28.06
6.	12	0.2	0.160	0.040	20.00

Table 1(b). Effect of pH on Cr^{6+} removal (%) by fRGO

Sl. no.	pH	Initial conc. of Cr^{6+} (mg/L)	Average effluent conc. of Cr^{6+} (mg/L)	Adsorbed conc. of Cr^{6+} (mg/L)	Cr^{6+} removal (%)
1.	2	0.2	0.063	0.132	65.85
2.	4	0.2	0.076	0.124	61.94
3.	6	0.2	0.092	0.108	54.10
4.	8	0.2	0.104	0.096	48.11
5.	10	0.2	0.124	0.076	37.97
6.	12	0.2	0.156	0.044	22.07

(GO). These functional groups contribute significantly to the sorption capacity by forming complexes with the metal ions[27]. Furthermore, in case of iron functionalized reduced graphene (fRGO) more and more Cr^{6+} adsorbed as pH is lowered. At a low pH (around 2) Cr^{6+} exists in $HCrO_4^-$, whereas iron in

fRGO remains positively charged (Fe^{3+}/Fe^{2+}). Due to coexistence of these two oppositely charged spices at lower pH the electrostatic interaction between them become predominant, and thus higher and higher takes place at lower pH. According to Eh-pH diagram, Cr^{6+} form CrO_4^{2-} at a pH of 6.5 and above. At the same time graphene and graphene oxide composite have iso-electric point at a pH of 3.3. Thus, at pH 8 both are negatively charged.

Hence, due to repulsive force between adsorbent surface and CrO_4^{2-} adsorption reduces. The iron on the functionalised fRGO can form metal oxides or hydroxides. These metal oxides/hydroxides can be protonated at lower pH and subsequently acquired positive charge[28]. At lower pH, the Cr^{6+} forms $HCrO_4^-$ which is attracted by fRGO nano composite and shows increased removal[26].

Adsorption isotherm:

The effect of adsorbent dose on Cr^{6+} removal data is shown in Table 2(a) and in Table 2(b). From this result it is clear that with increasing dose of GO and fRGO, the percent removal of Cr^{6+} was increased and for each dose of GO and fRGO % removal of Cr^{6+} is higher in the case of fRGO.

Table 2(a). Effect of adsorbent dose (GO) on Cr^{6+} removal (%) pH = 2.0

Sl. no.	Dose of fRGO (mg)	Initial conc. of Cr^{6+} (mg/L)	Average effluent conc. of Cr^{6+} (mg/L)	Adsorbed conc. of Cr^{6+} (mg/L)	Cr^{6+} removal (%)
1.	0	0.2	0.080	0.12	60
2.	20	0.2	0.064	0.136	68.75
3.	40	0.2	0.036	0.164	82.1
4.	60	0.2	0.016	0.184	92
5.	80	0.2	0.0097	0.1903	95.13
6.	100	0.2	0.0074	0.1926	96.32

Table 2(b). Effect of adsorbent dose (fRGO) on Cr^{6+} removal (%)

Sl. no.	Dose of fRGO (mg)	Initial conc. of Cr^{6+} (mg/L)	Average effluent conc. of Cr^{6+} (mg/L)	Adsorbed conc. of Cr^{6+} (mg/L)	Cr^{6+} removal (%)
1.	0	0.2	0.07	0.130	65
2.	20	0.2	0.045	0.155	77.3
3.	40	0.2	0.017	0.183	91.6
4.	60	0.2	0.009	0.191	95.65
5.	80	0.2	0.007	0.193	96.58
6.	100	0.2	0.005	0.195	97.22

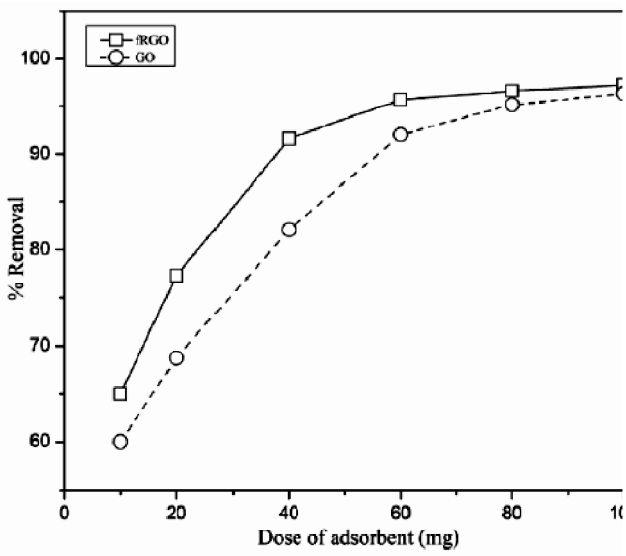

Fig. 3. Effect of adsorbent dose on Cr^{6+} removal. pH = 2.

Fig. 3 shows the effect of adsorbent dose (GO and fRGO) on Cr^{6+} removal. It is clear that with increasing dose for both the adsorbents, removal increases. Further, for all the doses of both the materials, fRGO performs better than GO. For the present study with Cr concentration of 0.2 mg/L at a pH of 2, the removal becomes asymptotic after an adsorbent dose of 100 mg/100 mL.

The adsorption data was then fitted to obtain isotherms model. Two basic adsorption isotherms namely Freundlich and Langmuir isotherms were investigated for Cr^{6+} removal by both GO and fRGO. For characterizing the single layer adsorption morphology, the Langmuir adsorption isotherm is used, whereas the Freundlich adsorption isotherm characterize a heterogeneous surface with intermediary and low adsorbate concentrations[18,19].

The following linear equation represents the Langmuir adsorption isotherm

$$1/q = 1/ (q_{max}\, C\, K_L) + 1/q_{max} \quad (1)$$

where, C (mg/L) is the equilibrium solute concentration, q (mg/g) is the equilibrium adsorption capacity, q_{max} (mg/g) is the maximum adsorption capacity, and K_L (L/mg) is the Langmuir constant which is related to the intensity of adsorption. A plot of Langmuir isotherm model ($1/q$ vs $1/C$) for Cr^{6+} removal by GO and fRGO is shown in Fig. 4. The maximum adsorption capacity, q_{max} for both the adsorbent GO and fRGO were found to be 9.80 mg/g and 17.30 mg/g respectively.

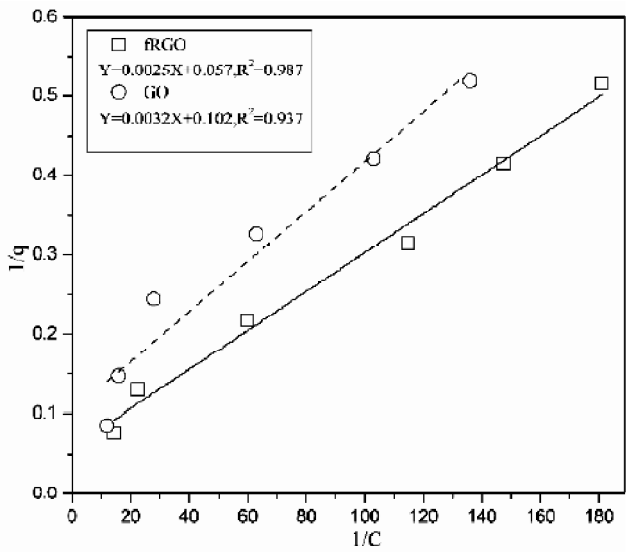

Fig. 4. Langmuir adsorption isotherm model.

The Freundlich adsorption isotherm is represented by the following equation,

$$\log q_e = \log K_F + 1/n \log C_e \quad (2)$$

where q_e (mg/g) = equilibrium adsorption capacity, K_F (mg/g) = adsorption capacity, n (L/g) = adsorption intensity and C_e (mg/L) = equilibrium concentration. A plot of Freundlich adsorption isotherm model of Cr^{6+} removal by GO and fRGO is shown in Fig. 5.

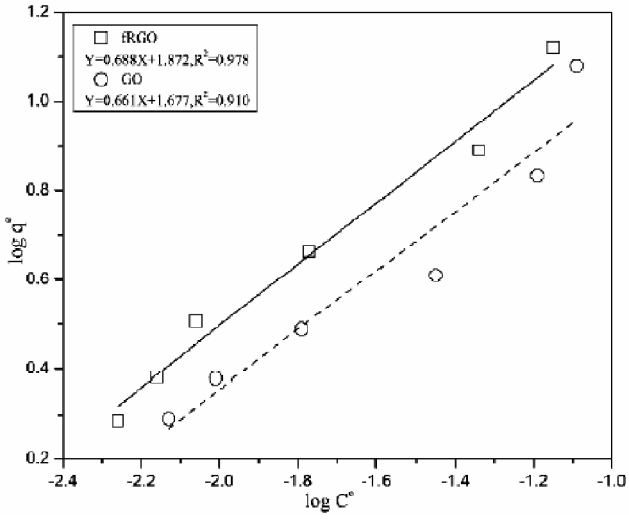

Fig. 5. Freundlich adsorption isotherm model.

It is clear from the plot that Langmuir isotherm plot fits better than Frundlich isotherm. For GO and fRGO the adsorption capacities for Freundlich isotherm (K_F) are found to be 48.19 mg/g and 73.79 mg/g respectively. The model fitness (R^2) and other constants are presented in Table 3. It was found that Langmuir isotherm fits better than Freundlich isotherm for both GO and fRGO and adsorption capacity (q_{max}) of fRGO (17.30 mg g^{-1}) is 1.76 times more than GO (9.80 mg g^{-1}). To ascertain the spontaneity of adsorption process, free energy of adsorption for the two materials were calculated using the following equation.

Table 3. Langmuir and Frundlich isotherm constants

	Langmuir isotherm			Freundlich isotherm		
Adsorbent	q_{max}	K_L	R^2	K_F	n	R^2
GO	9.80	32.90	0.934	48.19	1.51	0.909
fRGO	17.30	24.08	0.985	73.79	1.46	0.978

$$\Delta G = -RT \ln K \quad (3)$$

where ΔG is the Gibbs free energy, T is the absolute temperature (K), R is the gas constant (8.314 J/mol K), K is the Langmuir isotherm constant.

Free energy for fRGO and GO at experimental condition (25°C) are found to be –8158.32 J/mol and –6481.17 J/mol respectively. The negative values of ΔG signifies that the adsorption processes were spontaneous for both GO and fRGO.

Kinetic study:

The effect of contact time on Cr^{6+} removal was conducted by varying the time ranging from 10 min to 240 min. Removal of Cr^{6+} seemed to take place in two different phases. The experimental result is shown in Table 4(a) and Table 4(b).

Table 4a. Effect of contact time on Cr^{6+} removal (%) by GO

Sl. no.	Time (min)	Initial conc. of Cr^{6+} (mg/L)	Average effluent conc. of Cr^{6+} (mg/L)	Adsorbed conc. of Cr^{6+} (mg/L)	Cr^{6+} removal (%)
1.	10	0.2	0.180	0.02	10
2.	30	0.2	0.150	0.05	25
3.	60	0.2	0.119	0.0811	40.55
4.	90	0.2	0.075	0.125	62.5
5.	120	0.2	0.072	0.128	64
6.	150	0.2	0.057	0.143	71.5
7.	180	0.2	0.039	0.161	80.5
8.	240	0.2	0.022	0.178	88.9

Table 4b. Effect of contact time on Cr^{6+} removal (%) by fRGO

Sl. no.	Time (min)	Initial conc. of Cr^{6+} (mg/L)	Average effluent conc. of Cr^{6+} (mg/L)	Adsorbed conc. of Cr^{6+} (mg/L)	Cr^{6+} removal (%)
1.	10	0.2	0.07	0.130	65
2.	30	0.2	0.045	0.155	77.3
3.	60	0.2	0.017	0.183	91.6
4.	90	0.2	0.009	0.191	95.65
5.	120	0.2	0.007	0.193	96.58
6.	150	0.2	0.005	0.195	97.22
7.	180	0.2	0.07	0.130	65
8.	240	0.2	0.045	0.155	77.3

Initial phase involved rapid Cr^{6+} adsorption within 1 h followed by slower adsorption of Cr^{6+}. Adsorption kinetics is assumed rapid because GO and fRGO adsorbed 40.15% and 67.5% Cr^{6+} respectively within 1.5 h of contact time.

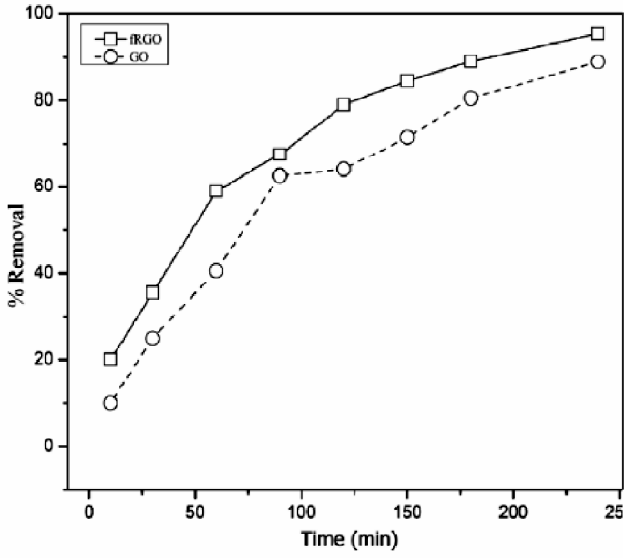

Fig. 6. Cr^{6+} removal (%) with variation of time (min).

Equilibrium is achieved after 4 h of contact time. At equilibrium the removal efficiency of Cr^{6+} for GO and fRGO are 88.9% and 95.25% respectively. Even though the surface of GO and fRGO are non-porous, due to presence of large surface area, the initial adsorption on the vacant surface is high[29].

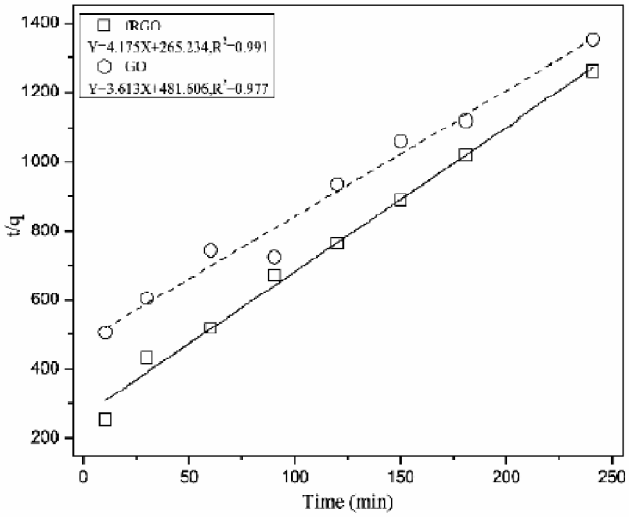

Fig. 7. Pseudo-second order model.

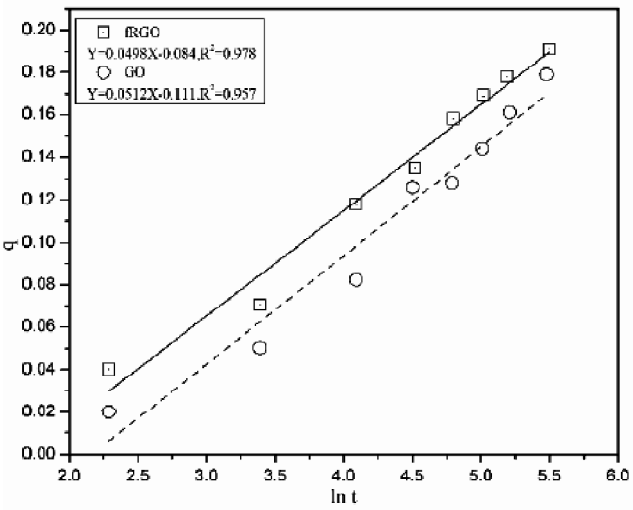

Fig. 8. Elovich model.

Elovich model:

$$q_t = \ln(\alpha\beta) + 1/\beta \ln t \quad (5)$$

where α (mmol/g/h) is the initial adsorption rate and β (g/mmol) is the desorption rate constant. Elovich model is shown in Fig. 8.

Intraparticle diffusion model:

$$q_t = K_{diff}\, t^{0.5} + C \quad (6)$$

where, K_{diff} (mg/g.$h^{-0.5}$) is the intraparticle diffusion rate con-

stant and *C* (mg/g) is a constant. Intraparticle diffusion model are shown in Fig. 9.

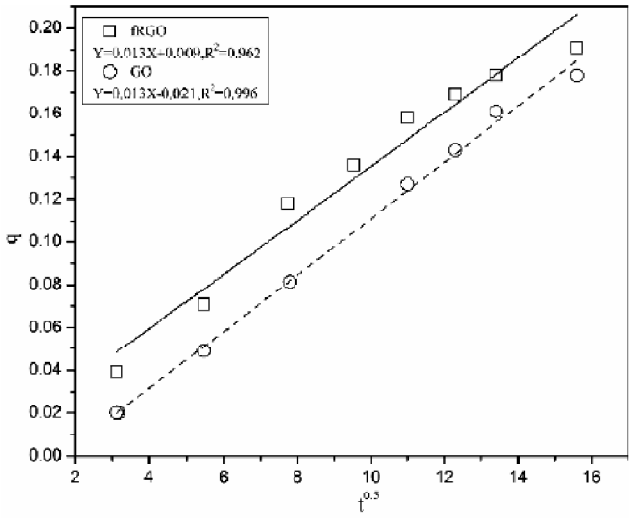

Fig. 9. Intraparticle diffusion model.

It is clear from Table 5 we have seen that pseudo-second order model is best fitted on the experimental data point for both the cases which implies that the phenomenon of adsorption is chemisorption.

Table 5. Kinetic constants

Adsorbent	Pseudo-second order model			Dlovich model			Intraparticle diffusion	
	q_e	*K*	R^2	α	β	R^2	*K*	*C*
GO	0.27	0.03	0.97	0.05	19.6	0.95	0.01	0.01
fRGO	0.24	0.07	0.99	0.05	20	0.98	0.01	0.02

Conclusions

It is observed from this study that both GO and fRGO can remove Cr^{6+} effectively from contaminated water. Comparative to the two materials fRGO performs better that GO. When graphene oxide is reduced to reduce graphene oxide (RGO) then the hydrogen ions are increased in molecule. This enhancement is helpful to functionalized with iron and it rapidly increase chemisorption with the ligand like Cr^{6+} from contaminated water. This nano adsorbent is useful for Cr^{6+} treatment with small footprint and efficient removal. The optimum pH of the system was found to be at a pH of 2 which can be directly used to treat acidic industrial wastewater like chrome plating industry. However, more studies still require optimizing the system with multivariate analysis to suggest interactions among the factors and a mathematical model to predict removal performance.

References

1. WHO, Chromium, Environmental Health Criteria 61, World Health Organization, Geneva, 1988.
2. Z. Kowalski, *J. Hazard. Mater*., 1994, **37**, 137.
3. G. Saner, Alan R. Liss, New York, 1980.
4. L. Dupont and E. Guillon, *Environmental Science & Tech*., 2003, **37**, 4235.
5. Marvin J. Udy, New York Reinhold Publishing Co., 1956.
6. I. Ali, *Chem. Rev.*, 2012, **112**, 5073.
7. V. Sarin and K. Pant, *Bioresource Tech*., 2006, **97**, 15.
8. E. Alvarez-Ayuso, A. Garcıa-Sánchez, X. Querol, *Water Research*, 2003, **37**, 4855.
9. F. N. Acar and E. Malkoc, *Bioresource Tech*., 2004, **94**, 13.
10. N. Kongsricharoern and C. Polprasert, *Water Science and Tech*., 1996, **34**, 109.
11. L. Monser and N. Adhoum, *Sep. Purif. Technol*., 2002, **26**, 137.
12. A. Hafez and S. El-Mariharawy, *Desalination*, 2004, **165**, 141.
13. S. Rengaraj, C. K. Joo, Y. Kim and J. Yi, *J. Hazard. Mater*., 2203, **102**, 257.
14. S. Rengaraj, K. H. Yeon and S. H. Moon, *J. Hazard. Mater.*, 2001, **87**, 273.
15. S. Dahbi, M. Azzi and M. De la Guardia, *Fresenius' J. of Analytical Chemistry*, 1999, **363**, 404.
16. V. K. Gupta and I. Ali, *J. of Colloid and Interface Science*, 2004, **271**, 321.
17. S. E. Bailey, T. J. Olin, R. M. Bricka and D. D. Adrian, *Water Research*, 1999, **33**, 2469.
18. L. Li, L. Fan, M. Sun, H. Qiu, X. Li, H. Duan and C. Luo, *Colloids and Surfaces B: Biointerfaces*, 2013, **107**, 76.
19. K. Li, P. Li, J. Cai, S. Xiao, H. Yang and A. Li, *Chemosphere*, 2016, **154**, 310.
20. H. R. Nodeh, W. A. W. Ibrahim, I. Ali and M. M. Sanagi, *Environmental Science and Pollution Research*, 2016, **23**, 9759.
21. R. F. Curl, R. E. Smalley, H. W. Kroto, S. O'Brien and J. R. Heath, *J. of Molecular Graphics & Modelling*, 2001, **19**, 185.
22. S. Ghosh, S. K. Ray and C. Majumder, *J. Indian Chem. Soc*., 2019, **96**, 435.
23. K. Hristovski, A. Baumgardner and P. Westerhoff, *J. Hazard. Mater*., 2007, **147**, 265.
24. K. Zhang, V. Dwivedi, C. Chi and J. Wu, *J. Hazard. Mater.*,

2010, **182**, 162.

25. W. S. Hummers (Jr.) and R. E. Offeman, *J. Am. Chem. Soc*., 1958, **80**, 1339.
26. S. K. Ray, C. Majumder and P. Saha, *RSC Adv.*, 2017, **7**, 21768.
27. R. K. Upadhyay, N. Soin and S. S. Roy, *RSC Adv*., 2014, **4**, 823.
28. W. Stumm, John Wiley & Son Inc., 1992
29. K. Pillay, E. M. Cukrowska and N. J. Coville, *J. Hazard. Mater.*, 2009, **166**, 1067.